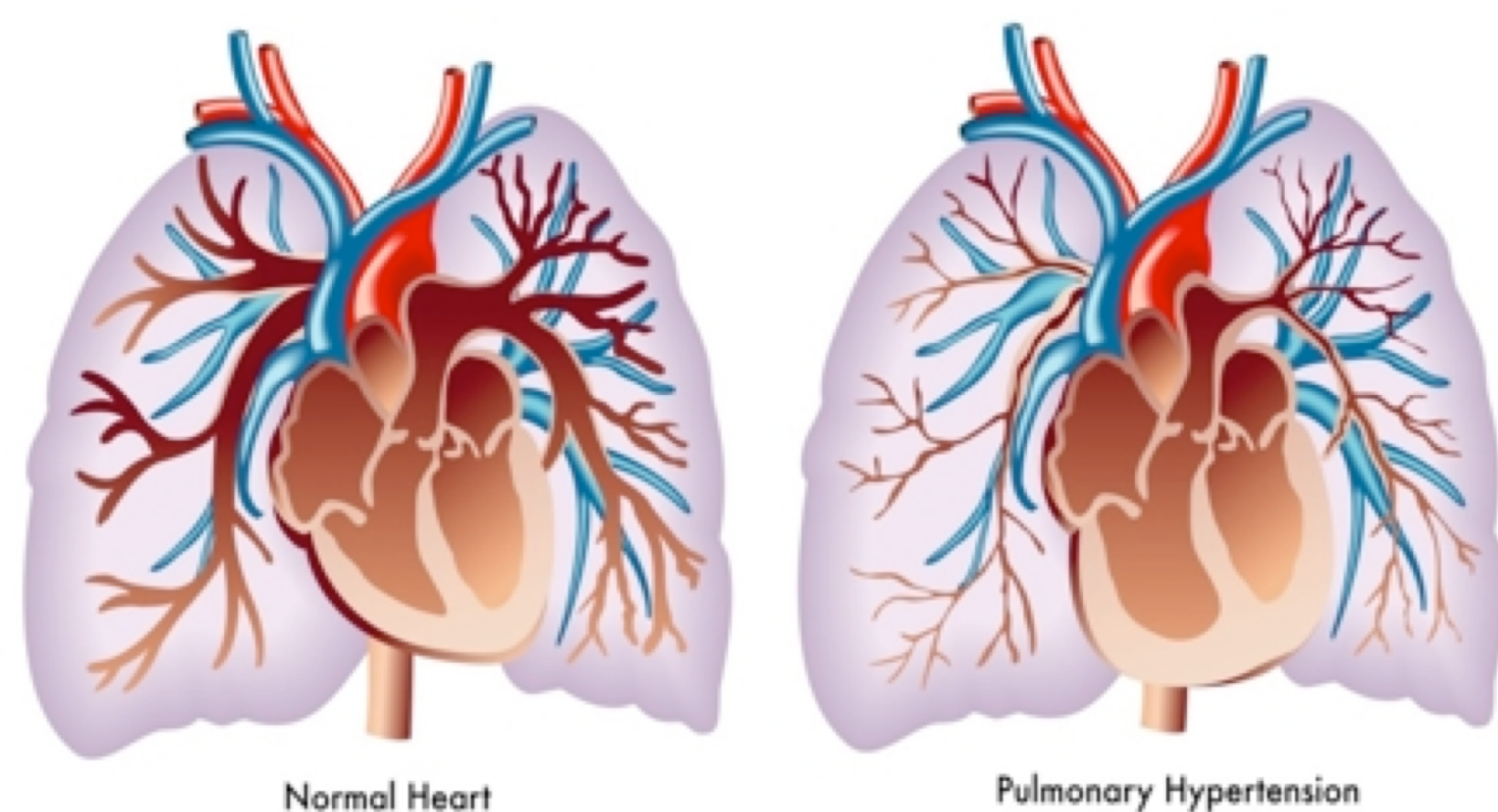
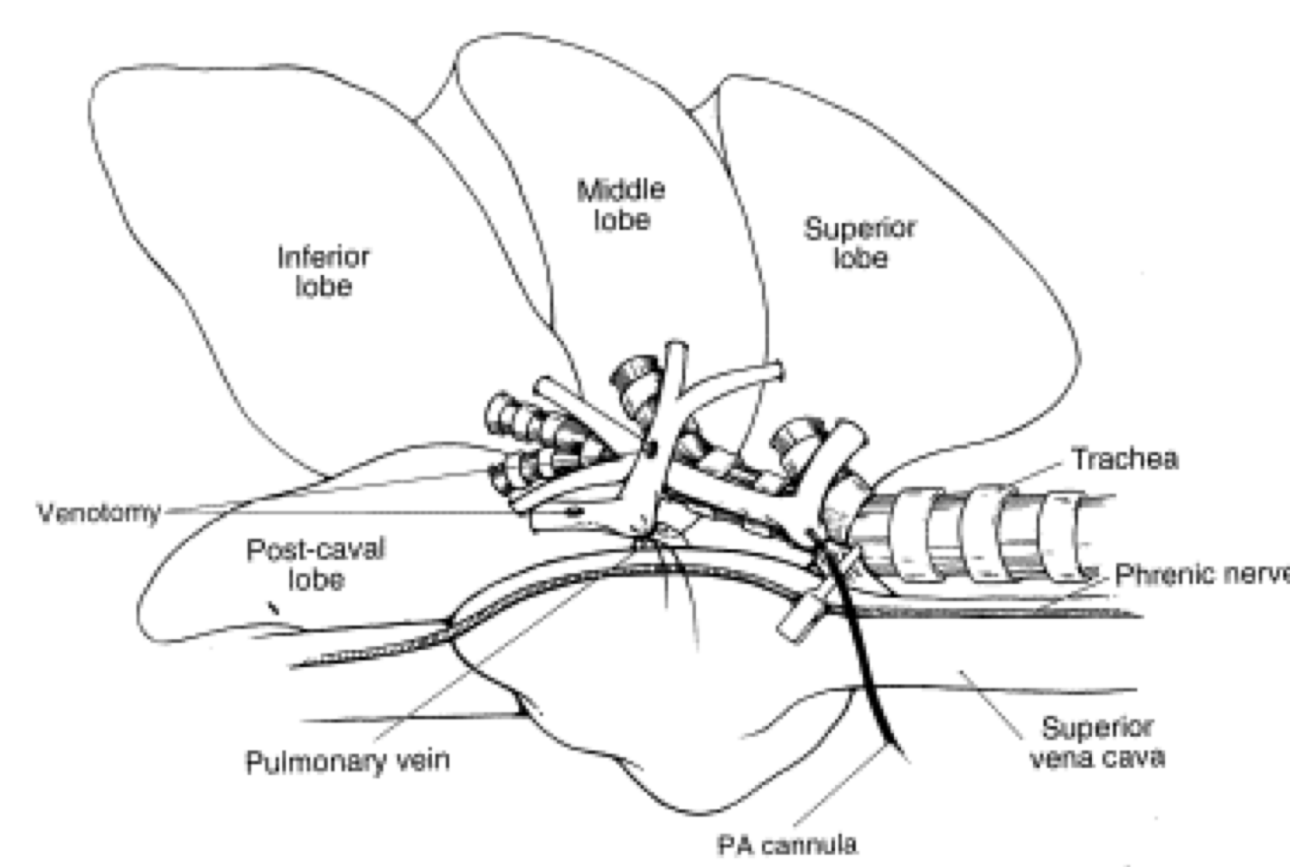


## I. INTRODUCTION

- Pulmonary arterial hypertension (PAH) often occurs in idiopathic forms and is commonly associated with disease including cirrhosis, congenital health malformation, and scleroderma.
- A clinical manifestation of chronic PAH is the progressive pruning of pulmonary blood vessels which often leads to death from heart failure
- The ability to better quantify the progression of vascular changes is hoped to improve outcomes for patients and accelerate the translation of future PAH-correction agents to the clinic.
- In-house software tools have been developed to characterize pulmonary vasculature non-invasively from chest CT images.



**Figure 1:** PAH in humans results in observable vascular changes including loss (pruning) of smaller arterioles and enlarged right ventricle of the heart.<sup>1</sup>



**Figure 2:** Lung anatomy in the rat includes 4 lobes in the right hemi-lung and a prominent central pulmonary artery (PA).

### OBJECTIVE :

To quantify pulmonary vasculature changes in PAH-induced rat models treated/not treated with an experimental drug compared with healthy controls.

## II.METHODOLOGY: IMAGING AND SEGMENTATION

### IMAGE ACQUISITION

- A left pneumonectomy was performed on the rat and after 7 days of recovery<sup>2</sup>, PAH was induced by injection of monocrotaline (MCT, 50 mg/kg)<sup>3</sup>. At 11 days post-MCT injection, the rats were anesthetized, the aorta transected, and the right hemi-lung flushed with a phosphate buffered saline and nitric oxide donor to promote vasodilation.
- A solution of 30% barium sulfate (imaging contrast agent) agarose was injected into the main right pulmonary trunk. The hemi-lung was then inflected with 10% formaldehyde and the right middle lobe was harvested (1 of 4 lobes in the right lung), and placed in ice.
- The viscosity of the agarose gel limits its extension to 30- $\mu$ m vessels.
- The right middle lobe (Sprague Dawley rats have 4 lobes in the right hemi-lung) was isolated and scanned for 8 hours at 15- $\mu$ m isotropic resolution on a desktop micro-CT imaging system.<sup>4</sup> The images were down-sampled to 30- $\mu$ m isotropic voxels to reduce computational resources.

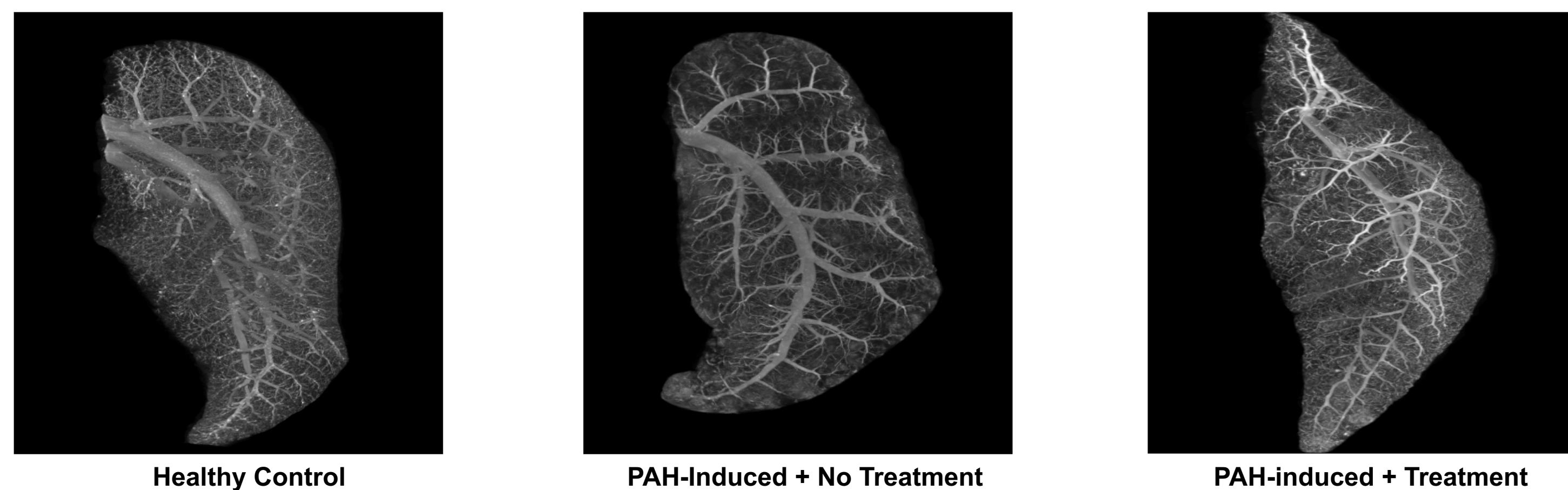


**Figure 3:** Shown are maximum intensity projections (MIP) of the micro-CT data sets of the rat right middle lobe from a control [left], a PAH-induced [middle], and a PAH-induced + treatment [right] rats. A low viscosity agarose gel infused with Barium-sulfate projected contrast enhancement of the arterial tree down to 30  $\mu$ m.

### LUNG VESSEL SEGMENTATION

- In-house software built upon the NIH ImageJ platform was used to first extract the vascular structures from the micro-CT datasets of the right hemi-lung middle lobe using a region-growing method starting from a manually-selected seed point.<sup>5</sup>
- Next, the software computed the number of blood vessel branches and their radii.
- Skeletonizing was applied to facilitate traversing and characterizing the tree structure. The radius and length of each branch were then computed.
- This approach was applied to nine rat lung CT datasets: 3 healthy controls, 4 PAH-induced at a single time after injury, and 2 PAH-induced with an administered experimental drug.

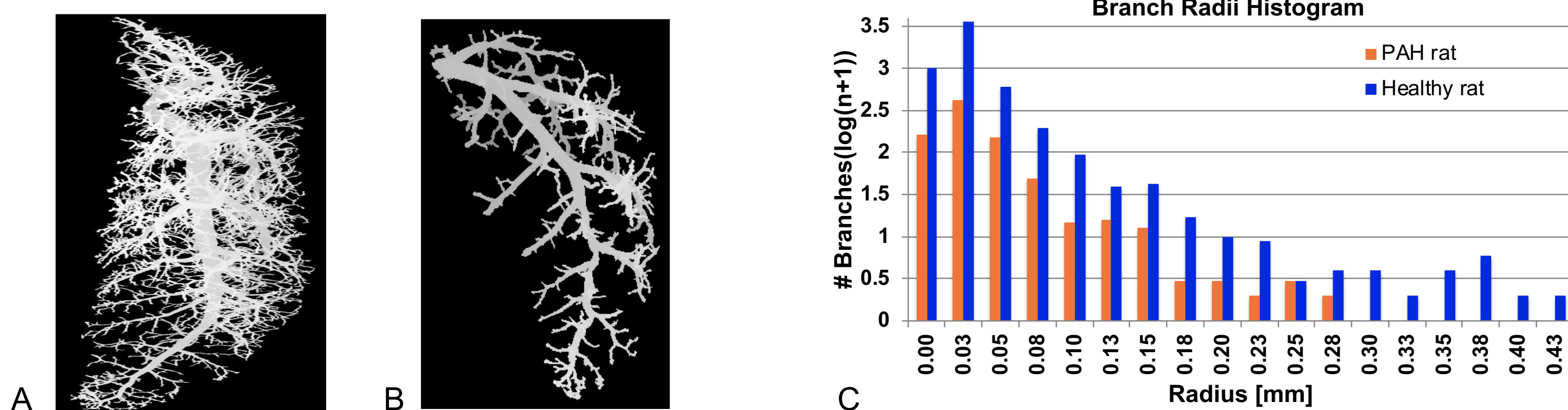


**Figure 4:** Histogram of branch number versus branch radius for control and PAH rat lungs. Shown in [A] and [B] are the extracted vascular trees of a healthy and PAH-induced rat. [C] shows the branch radius histogram for the same rat lungs. On this log scale it is expected that as the radius decrease the number of branches increases linearly. The characteristic holds in both lungs for branches down to 25  $\mu$ m in radius (50  $\mu$ m diameter), roughly 2x the isotropic pixel dimensions (23.7  $\mu$ m) of the resolution-adjusted micro-CT scans acquired in these isolated lungs.

## ACKNOWLEDGEMENTS

Funding for this work is provided by the UF Department of Radiation Oncology and UF University Scholars Program.

## III. RESULTS AND DISCUSSION

### RESULTS

- Figure 5 plots the number of branches for each experimental animal, segregated by intervention.

### STATISTICAL ANALYSIS

- The mean  $\pm$  standard deviation of the total number of vessel branches for each cohort were 12608  $\pm$  63 (healthy controls, 5502  $\pm$  1134 (PAH-induced with no post-drug) and 11843  $\pm$  944 (PAH-induced with post-drug).
- Multiple t-tests were used to compare statistical significance of the number of vessel branches extracted between the three cohorts:
- Healthy controls and PAH-induced without post treatments cohorts were significantly different ( $p=0.001 < \alpha(0.05)$ ).
- PAH-induced with and without treatments were significant ( $p= 0.005 < \alpha(0.05)$ ).
- Healthy controls and PAH-induced with post treatment cohorts were not significantly different ( $p= 0.46 > \alpha(0.05)$ ).
- This demonstrated the possible efficiency of the experiment drug intervention to promote the normal restoration of the pulmonary vasculature.

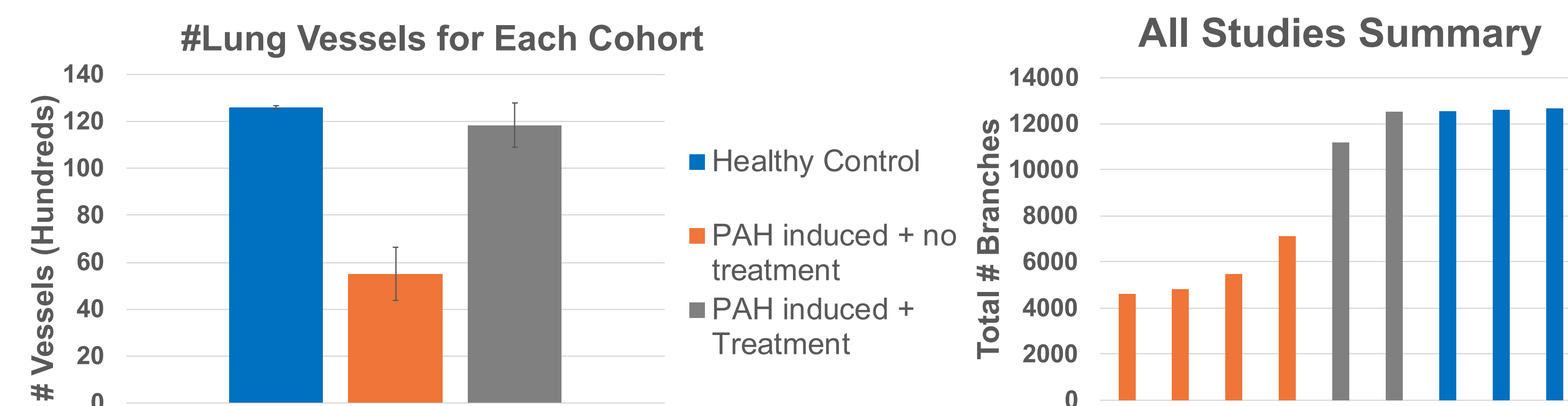


**Figure 5:** The leftmost graph shows the averages for the distribution of total number of arterial branches across 9 rat right middle lobes, segregated by each experimental group. The right graph shows the individual distribution of the total number of arterial branches across the 9 lobes.

### DISCUSSION

- The main experimental challenge with this study was the variable quality of vessel appearance. Some scans exhibited less prominent vessel contrast, leading to the need to apply a lower initial threshold for vessel extraction.
- There were gaps in the vessel lumens in approximately 75% of the scans, usually in large vessels at bifurcations. This was due to the shrinkage of the agarose-gel.
- A software tool was created to assist in the manual editing of the images using filled ellipses to enable a more complete characterization of the vascular tree networks.

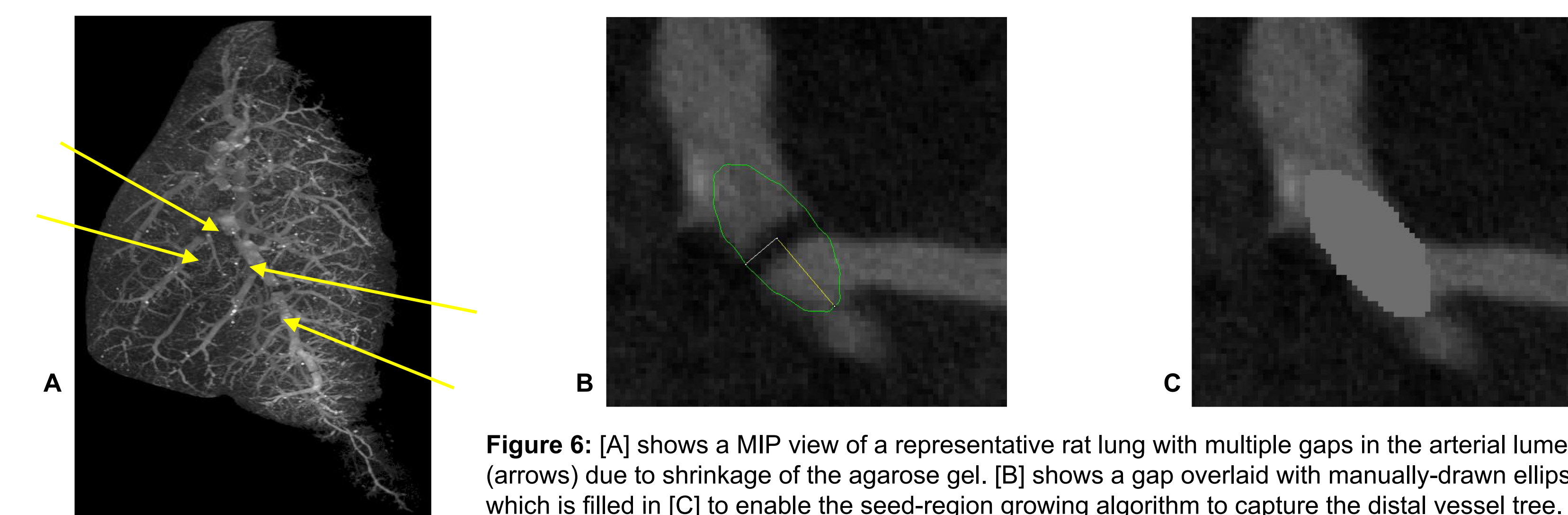


**Figure 6:** [A] shows a MIP view of a representative rat lung with multiple gaps in the arterial lumen (arrows) due to shrinkage of the agarose gel. [B] shows a gap overlaid with manually-drawn ellipse which is filled in [C] to enable the seed-region growing algorithm to capture the distal vessel tree.

- The large file size of the micro-CT data sets made the analysis computationally intensive.
- Even after reducing the resolution of the original CT data by half in each direction (1/8 size in total), a typical data set consisted of about 2,400 images, requiring greater than 10 Gigs of RAM when run through the ImageJ software.

## IV. CONCLUSION

- The experimental models of PAH and intervention produced a broad spectrum of vascular changes, and our tools for the extraction and characterization of vessels from CT images likewise reflected such a spectrum.
- Our data shows three groups of the total number of branches that can be attributed to the three experimental rat lung groups.
- Plans for future work are to adjust more accurately for the gaps to account for some drops in the vessel count.
- The experiments produce widely differing stages of vascular pruning, and our objective analysis reflects this disparity.

## IV. REFERENCES

1. Moore C, New Survey Finds People With Pulmonary Hypertension Face Serious Health, Social And Financial Impacts. CTEPH News, PAH News. (2014).
2. Nawata, Sumihiko, Amir Abolhoda, Howard M. Ross, Ari Brooks, and Michael E. Burt. "Sequential bilateral isolated lung perfusion in the rat: an experimental model." *The Annals of thoracic surgery* 63, no. 3 (1997): 796-799.
3. Kasahara, Y., Kiyatake, K., Tatsumi, K., Sugito, K., Kakusaka, I., Yamagata, S., Ohmori, S., Kitada, M., and Kuriyama, T., Bioactivation of monocrotaline by p-450 3a in rat liver. *Journal of Cardiovascular Pharmacology*, 1997. 30(1): p. 124-9.
4. Langheinrich, A.C., Leithauser, B., Greschus, S., Von Gerlach, S., Breithecker, A., Matthias, F.R., Rau, W.S., and Bohle, R.M., Acute rat lung injury: Feasibility of assessment with micro-ct. *Radiology*, 2004. 233(1): p. 165-71.
5. O'Dell W, Gormaley A, Prida D., Validation of the Gatorial Method for Accurate Sizing of Pulmonary Vessels from #D Medical Images. *Medical Physics*, 2017;44.